Journal of Organometallic Chemistry, 449 (1993) 95–104

JOM 23368

Indium tert-butylthiolates as single source precursors for indium sulfide thin films: is molecular design enough?

Andrew N. MacInnes [a], Michael B. Power [a,b], Aloysius F. Hepp [b] and Andrew R. Barron [a]

[a] *Department of Chemistry, Harvard University, Cambridge MA 02138 (USA)*
[b] *NASA, Lewis Research Center, Cleveland, OH 44135 (USA)*

(Received August 3, 1992)

Abstract

The dimeric indium thiolates $[R_2In(\mu\text{-}S^tBu)]_2$ R = ^{t}Bu (**1**), ^{n}Bu (**2**), Me (**3**), and $[(^tBuS)MeIn(\mu\text{-}S^tBu)]_2$ (**4**) have been synthesized and used as single source precursors for the metal-organic chemical vapor deposition (MOCVD) of In/InS and InS thin films. In the case of the atmospheric pressure film grown from either **1** or **2**, deposition at temperatures between 290 and 350°C results in the formation of indium rich films (In : S ~ 2) consisting of indium metal and orthorhombic InS, while at 400°C a single phase; the tetragonal high pressure phase of InS, is the only product deposited. Use of compound **3** as the precursor results in amorphous indium rich films being deposited at 300°C. While films grown from **3** at 400°C have a In : S ratio of 1, they consist of an indium rich phase and In_2S_3. The dependence of the film composition *i.e.*, indium rich *versus* stoichiometric InS and structure (orthorhombic *versus* tetragonal InS) with the deposition temperature and molecular precursor is discussed with respect to the decomposition pathways available to the precursor molecules (**1–3**). Based on these results compound **4** was proposed to be a suitable precursor for the low temperature deposition of stoichiometric InS, indeed its solid state pyrolysis does yield InS. However, although low pressure MOCVD using **4** yields amorphous films of stoichiometry InS, upon annealing β-In_2S_3 is formed as the crystalline phase. The efficacy of molecular design of solid state materials is discussed. The indium thiolates were characterized by ^1H and ^{13}C NMR spectroscopy and mass spectrometry. Analysis of the deposited films has been obtained by X-ray photoelectron spectroscopy (XPS) and transmission electron microscopy (TEM), with associated energy dispersive X-ray analysis (EDX).

1. Introduction

The low temperature controlled formation of solid state materials from organometallic precursors has been an area of exponential growth over the last twenty years. During this time much effort has been aimed at the development of new stable precursors, in particular those containing all the desired elements in a single molecule [1]. While an ever larger number of chemistry papers reporting new organometallic compounds have as their justification the possible application of organometallic chemistry to materials science, those papers in which any attempt is made to prepare the target solid state material is still in the minority. However, an increasing number of reports in what are traditionally chemistry journals now concern not only the synthesis of new compounds and their application as precursors to solid state materials, but also include studies of the dependence of the final materials phase [2–4], composition [5–6], and morphology [7,8] upon the structure and substituents of the precursor molecule, the deposition temperature and even the carrier gas. Such studies highlight the importance of gaining an intimate understanding of the pathway from molecules to materials, and question the commonly held misconception that synthesis of a precursor compound with the appropriate composition will result in the formation of the desired material.

The indium sulfides, InS and In_2S_3, are medium band gap semiconductors (2.44 and 2.07 eV respectively) [9], and are therefore considered to hold promise as optoelectronic and photovoltaic materials [10]. In addition, the monosulfide may find a possible applica-

---

Correspondence to: Professor A.R. Barron.

0022-328X/93/$6.00

tion as a passivation layer on InP devices [11], in an analogous manner to the results achieved with the passivation of GaAs by GaS [12]. It is with this latter application in mind that we have recently undertaken a study of the metal organic chemical vapor deposition (MOCVD) of InS thin films using alkyl indium thiolates as single source precursors. We have communicated elsewhere [4] that the dimeric indium thiolate $[(^tBu)_2In(\mu\text{-}S^tBu)]_2$ may successfully be used as a single source precursor for the atmospheric pressure MOCVD of polycrystalline tetragonal InS thin films. The formation of the high pressure phase of InS as opposed to the thermodynamic orthorhombic phase suggested that significant molecular control of the deposited phase was in evidence [4], *i.e.*, the designed molecular motif determined the composition and phase of the deposited film. Unfortunately, the deposition temperature employed (*ca.* 400°C) is in excess of the temperature at which InP loses phosphorus (*ca.* 350°C), thus precluding the successful surface passivation of InP under the reported conditions. We have therefore undertaken an investigation into the possibility of lowering the deposition temperature. In addition we have investigated the effects of the alkyl substituent on indium on the elemental composition and identity of the sulfide phase. These studies are reported herein.

2. Results and discussion

2.1. Precursors: design, synthesis and characterization

Our previous work [4] on single-source precursors for InS employed the monothiolate complex $[(^tBu)_2In(\mu\text{-}S^tBu)]_2$ (**1**), as we had found the gallium analog to be suitable for the deposition of hexagonal GaS films [13]. However, over the film growth time (*ca.* 60 min.), and at its sublimation temperature, 170–200°C, decomposition of **1** was observed. In order to circumvent this problem alternative substituents at indium were investigated. Given that Nomura *et al.* have reported that the n-butyl derivatives of indium thiolates are liquids or low melting solids [14] we chose $[(^nBu)_2In(\mu\text{-}S^tBu)]_2$ (**2**) as a possible precursor. The presence of β-hydrogens on the indium alkyl substituents for compounds **1** and **2**, and the similarity of the films prepared from either molecule (see below) prompted the investigation of a non β-hydrogen containing derivative, *i.e.*, $[Me_2In(\mu\text{-}S^tBu)]_2$ (**3**). Likewise, the loss of sulfur content during film deposition between 300 and 350°C (see below) suggested the use of a sulfur rich precursor molecule, $[(^tBuS)MeIn(\mu\text{-}S^tBu)]_2$ (**4**).

The synthesis of $[R_2In(\mu\text{-}S^tBu)]_2$, R = ^{t}Bu (**1**), ^{n}Bu (**2**), Me (**3**), is readily accomplished is high yield by the reaction of ^{t}BuSH with the appropriate trialkylindium compound in pentane (eqn. (1)).

$$InR_3 + {}^tBuSH \xrightarrow[\text{pentane}]{25°C} \tfrac{1}{2}[R_2In(\mu\text{-}S^tBu)]_2 + {}^tBuH$$

$$R = {}^tBu(\mathbf{1}),\ {}^nBu(\mathbf{2}),\ Me(\mathbf{3}) \qquad (1)$$

The bis-thiolate $[(^tBuS)MeIn(\mu\text{-}S^tBu)]_2$ (**4**) is prepared by the reaction of **3** with an excess of ^{t}BuSH (eqn. (2)).

$$[Me_2In(\mu\text{-}S^tBu)]_2 + {}^tBuSH \xrightarrow{\Delta} [({}^tBuS)MeIn(\mu\text{-}S^tBu)]_2 + MeH \qquad (2)$$

Compounds **1**, **3** and **4** are white crystalline solids, while **2** is a viscous distillable colorless liquid. Compounds **3** and **4** melt without decomposition at 80–81°C and 74°C respectively. Although the compounds are not pyrophoric they all decompose over a period of hours in moist air to liberate the thiol (**CAUTION**: tert-butylthiol is extremely pungent and toxic), and thus they should be handled and stored under a dry inert (N_2, Ar *etc.*) atmosphere.

The predominant (100%) peak in the mass spectra of **1–4** is that associated with a dimer (see Experimental section). However, low intensity peaks are observed in the spectra for **2** and **3** due to trimeric fragments. Based on the following reasoning we believe that these are due to recombination within the mass spectrometer. Firstly, the ^1H and ^{13}C NMR spectra of **2** and **3** show the presence of a single set of resonances. It has been shown that where equilibria between oligomeric forms of Group 13 heterocycles are present, the exchange is slow on the NMR time scale, thus allowing for the observation of all oligomers simultaneously [15,16]. Secondly, the solution molecular weight for **2** and **3** are like that of **1** and **4**, well within experimental error of the dimer (see Experimental section). Thirdly, by analogy with the tert-butoxide derivatives of aluminum, gallium and indium it is unlikely that the trimers would be stable due to steric congestion [15,17].

While the dimeric nature of **4** is implied from mass spectrometry and solution molecular weight (see Experimental section), at ambient temperature only one type of ^{t}Bu resonances are apparent in both the ^1H and ^{13}C NMR spectra of **4**. The implied rapid interchange of bridging and terminal groups is a common facet of Group 13 dimers [18].

Thermogravimetric Analyses (TGA) of compounds **1–3** were performed under an inert (dry argon) atmosphere, in order to determine the volatilization-decomposition window. As can be seen from Fig. 1 all the compounds sublime with decomposition; 220°C (**1**), 261°C (**2**) and 198°C (**3**). Given the above the following

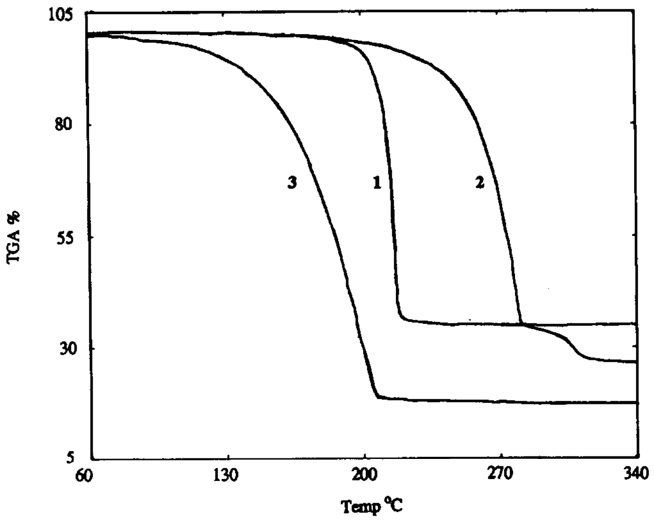

Fig. 1. The solid state thermal decomposition of the indium thiolate compounds $[R_2In(\mu\text{-}S^tBu)]_2$, R = ^{t}Bu (1), ^{n}Bu (2) and Me (3), as measured by their thermogravimetric analysis (TGA), see text for discussion.

volatilization temperatures were employed for the precursors: **1**, 170°C, **2**, 180–190°C, **3**, 110–120°C. Compound **4** does not show any volatility at atmospheric pressure, with thermolysis resulting in decompostion (see below).

2.2. *Thin film deposition studies*

Thin film growth using compounds **1**–**3** as precursors was carried out primarily on p-type (100) oriented silicon and single crystal KBr substrates in a resistively heated, horizontal, laminar flow glass MOCVD system operated at atmospheric pressure, as previously described [5]. Purified argon was used as a carrier gas. Additional studies using compound **1** as the precursor were carried out under vacuum (10^{-3} Torr) in a vertical reactor in which the heated substrate was suspended above the precursor (see Experimental section). The coatings adhered well to all substrates (Scotch Tape test). No appreciable difference in the film morphology as a function of substrate or deposition system was noted, however, the film composition and microstructure was found to be highly dependent on the identity of the precursor and the deposition temperature. This relationship is summarized in Table 1 and detailed below.

Films grown using either compounds **1** or **2** as the precursor at each of the temperatures 300 (±10)°C, 350 (±10)°C and 400 (±10)°C were essentially independent of the precursor in terms of morphology and phases present. The microstructural features and chemical composition of the deposited films were, however, observed to have significant dependence on the deposition temperature.

TABLE 1. Summary of the dependence of the In:S ratio and the crystalline phase with deposition temperature

Precursor	Deposition temp. (°C)	In:S ratio	Phases observed
1	300–350	2:1	orthorhombic InS + In rich amorphous phase
	400	1:1	tetragonal InS
2	300–350	2:1	orthorhombic InS + In rich amorphous phase
	400	1:1	tetragonal InS (highly oriented)
3	300–350	2:1	amorphous phase
	400	1:1	In_2S_3 and amorphous phase
4	300	1:1	amorphous phase, crystallizes to β-In_2S_3 upon annealing

Figure 2a shows the film obtained from precursor **1** grown at 300°C. The matrix phase yielded an amorphous electron diffraction pattern and was, by EDX

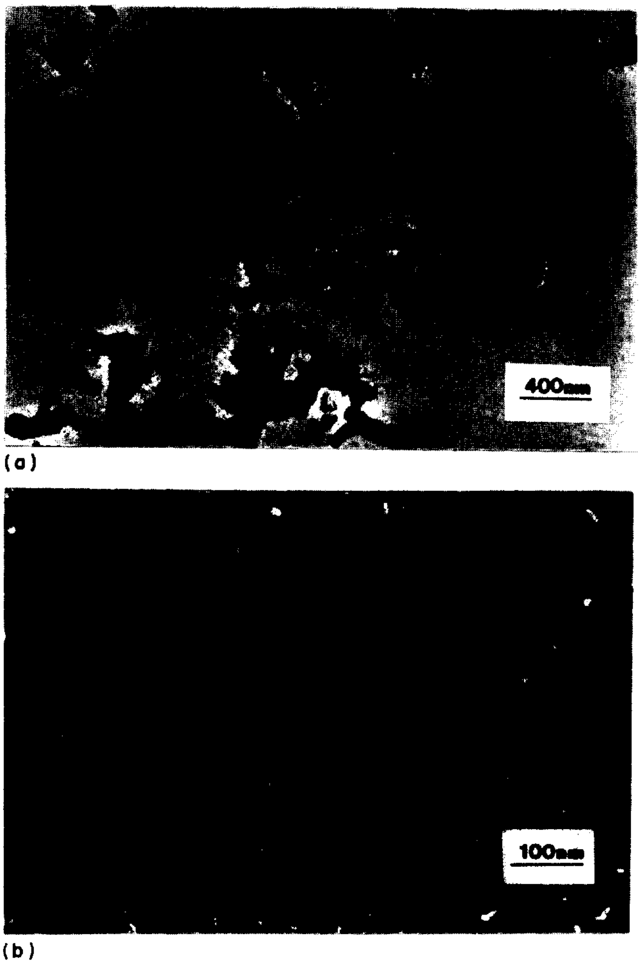

Fig. 2. Bright-field TEM image of films grown from $[(^nBu)_2In(\mu\text{-}S^tBu)]_2$ (**2**) at 300°C (a) and 400°C (b). Note the trigonal growth directions in the latter.

analysis, found to be predominantly indium in compositon with little or no sulfur (n.b. oxygen and other elements Z < 11 cannot be detected with this system). By similar analyses the island phase (darker) was found to be 50% In and 50% S (±2%) and furthermore exhibited an electron diffraction pattern consistent with orthorhombic InS [19]. (JCPDS#19-588). The overall composition of these films, as determined by EDX, was found to be in the region of *ca*. In 66%, S 33%. Films grown at 350°C using **1** and **2** as precursors were found to be similar in nature to those grown at 300°C.

Films from either **1** or **2** deposited at 400°C were found to be a single phase with distinct growth morphology, as indicated by the bright field TEM image shown in Fig. 2b. This type of film was identified previously by us [4] as being the tetragonal high pressure phase of InS (JCPDS#36-643) consistent with the observed electron diffraction (*e.g*., see Fig. 3) [20]. Thus, analysis of these films is in agreement with our earlier identification of a tetragonal InS film highly oriented in three mutually trigonal growth directions.

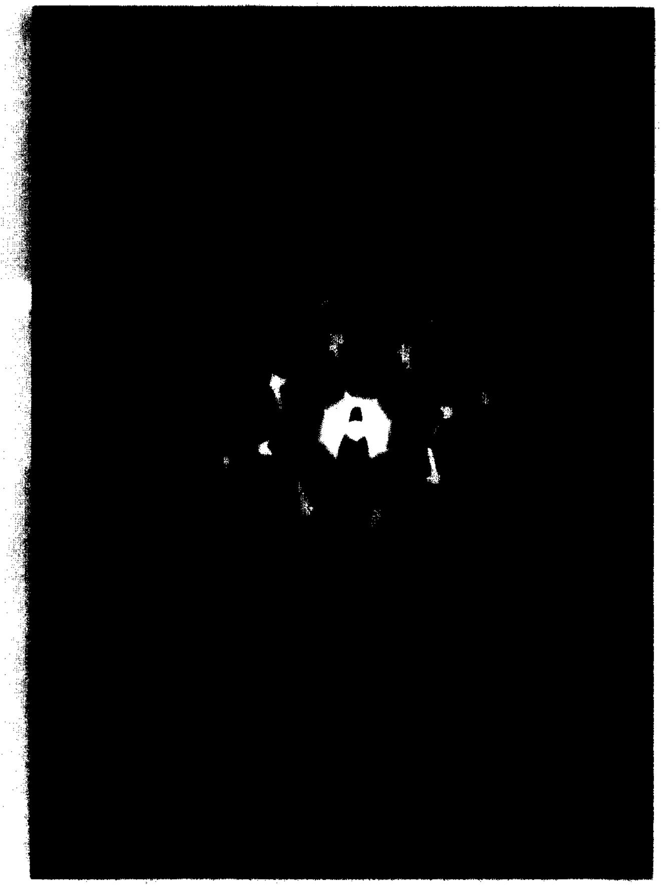

Fig. 3. Selected area diffraction pattern of the films grown from $[(^nBu)_2In(\mu\text{-}S^tBu)]_2$ (**2**) at 400°C, showing the formation of a single phase, tetragonal InS. Note the presence of a preferred orientation in the deposited films as indicated by diffraction spots as opposed to rings.

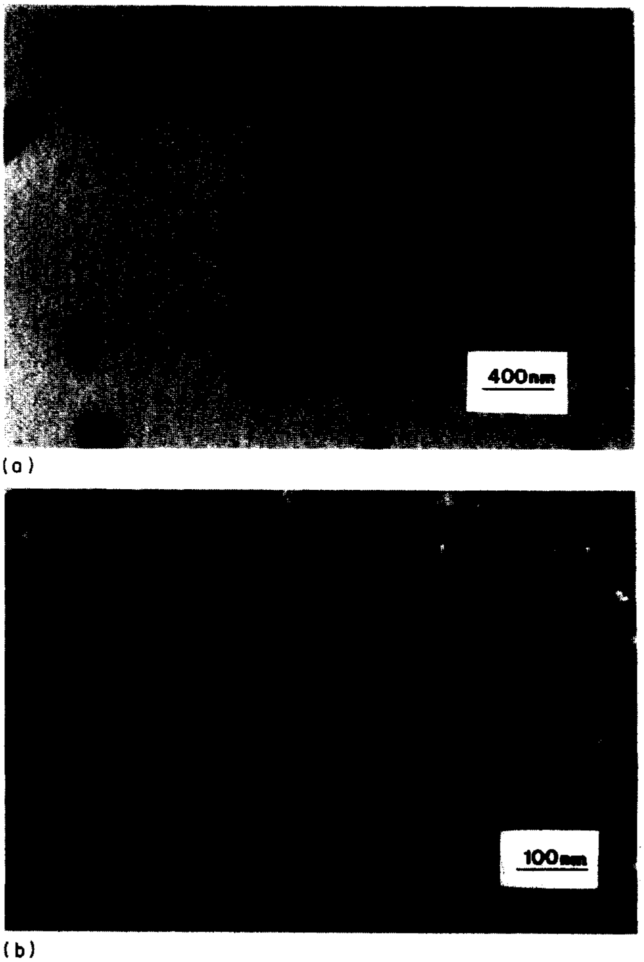

Fig. 4. Bright-field TEM image of films grown from $[Me_2In(\mu\text{-}S^tBu)]_2$ (**3**) at 300°C (a) and 400°C (b).

Films deposited from the methyl substituted precursor **3** show marked differences to those grown using **1** or **2**. At 300°C the morphology of the deposited film as shown in Fig. 4a consists of darker islands on what appears to be a generally featureless but 'speckled' background. The focusing of the electron probe of the microscope on these dark islands resulted in their disappearance revealing the featureless background. We therefore propose that these islands are either simply areas of residual precursor which have condensed on the coated substrates on cooling or carbon rich surface residues due to the precursor decomposition. EDX analysis indicated a film composition of In 65%, S 35% (±5%), with no obvious deviation from this value between any structural features including the dark islands analysed under conditions of low beam current to avoid evaporation. Electron diffraction yielded amorphous patterns for these films.

Films deposited from the methyl precursor **3** at 400°C, however, yielded a crystalline diffraction pattern superimposed on a background of broad amorphous rings (Fig. 5). The diffraction information obtained from these patterns indicates the presence of In_2S_3 (JCPDS#25–390) as the crystalline phase. Figure 4b shows the bright field image of the deposited film. Lighter coloured discs 20–40 nm in diameter may be observed on a background dotted with much smaller discs *ca*. 50 Å in diameter. EDX analysis of the overall film indicated a composition of 50% In and 50% S (±2%), which in light of the identification of In_2S_3 being present, would suggest that an indium rich phase should also be present. However, no evident deviation from the InS ratio of 1:1 could be detected in any of these morphological features identified.

X-ray photoelectron spectroscopy (XPS) indicated the absence of both carbon and oxygen in all films after a short argon ion sputter process designed to remove adventitious hydrocarbons and surface oxidation products. Higher resolution scans around the In3d$^{5/2}$ photoelectron peak, and In LMM auger peak were recorded to evaluate an auger parameter [21], α^* defined in this case as:

$$\alpha^* = \text{B.E. In } 3d^{5/2} + \text{K.E. In } L_4M_{45}M_{45} \qquad (3)$$

where B.E. = binding energy, K.E. = kinetic energy. Table 2 summarizes the recorded peak data and α^* values. It must be pointed out that the In LMM auger peak is very broad making the error in assignment of peak position sufficiently large as to make a strict distinction between the films based on α^* impossible. We may note, however, that the reported α^* values for InS are in the region of 853 eV whereas In_2S_3 and In_2O_3 are lower, being in the region of 852 eV [22].

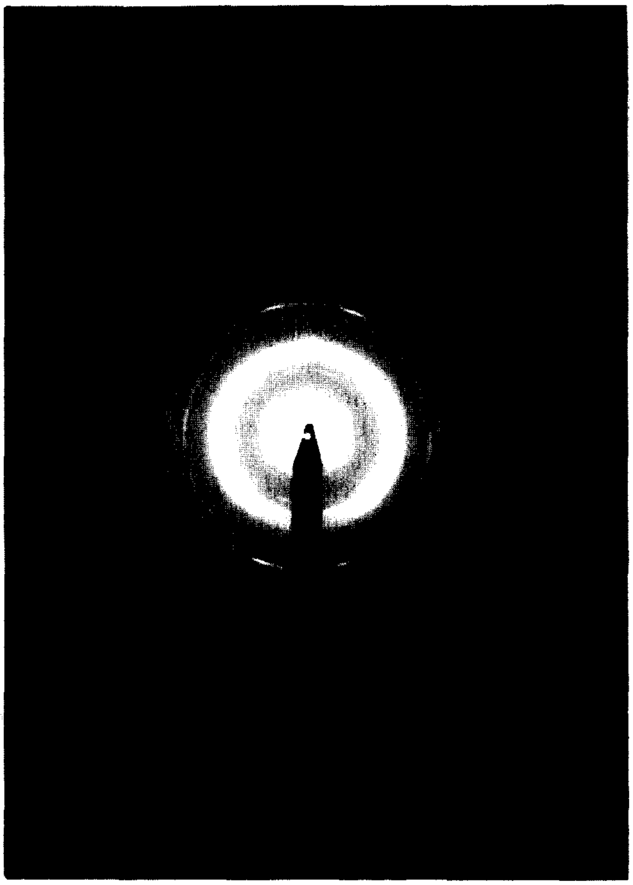

Fig. 5. Selected area diffraction pattern of the films grown from $[Me_2In(\mu\text{-}S^tBu)]_2$ (**3**) at 400°C, showing diffraction rings consistent with In_2S_3 superimposed on a broad amorphous halo.

TABLE 2. Auger parameter (α^*) evaluation for deposited films

Precursor	Deposition temp. °C	In3d$^{5/2}$ ±0.1 eV	In $L_4M_{45}M_{45}$ ±0.2 eV	α^* ±0.3 eV
1, 2	300	444.5	1078.8	852.4
	400	444.8	1078.2	853.1
3	300	444.8	1078.5	853.0
	400	445.0	1079.1	852.5
4	300	444.8	1078.9	852.5

As we have previously discussed [4], the formation of the high pressure tetragonal form of InS from compounds **1** and **2** upon deposition at 400°C is expected based upon the structural relationship of the molecular core and the atomic arrangement in the solid state, *i.e.*, retention of the In_2S_2 rings [4]. This precursor-phase dependence suggests that the dimeric molecule remains intact either upon loss of all, or some, of the organic substituents and/or deposition on the growth surface followed by subsequent loss of the organic species. In contrast, the films deposited from **1** and **2** at 300 and 350°C are indium rich, and contain the thermodynamically stable orthorhombic phase of InS suggesting fragmentation of the molecular precursor. This elemental imbalance cannot be due to loss of sulfur from the deposited film, since this would be expected to also occur at 400°C, which is clearly not the case. Thus, the loss of sulfur (*ca*. 50%) must be due to the temperature dependent nature of the decomposition pahtway.

Based upon GC/MS and ^{1}H NMR analysis of the condensible outflow from the depositions carried out at 300 and 350°C using **1** and **2**, the only sulfur-containing product is ^{t}BuSS^{t}Bu. While this may possibly be formed due to inter or intramolecular elimination we favor the former since the latter would result in the deposition of indium only. Likewise, if this reaction occurred in addition to deposition of InS then the tetragonal phase would still be observed. As a consequence of the loss of ^{t}BuSS^{t}Bu the deposited films would be expected to have a stoichiometry of In_2S, as is observed. While the In_2S molecule has been detected in the gas phase [23], and several groups [24] have postulated its existence as a solid state phase, Duffin and Hogg [25] have shown that In_2S is actually a mixture of In and InS. Our characterizations of the films deposited from **1** and **2** at 300 and 350°C are in full agreement with, and support, this result, whilst those from **3** at 300° display the correct In_2S stoichiometry despite yielding amorphous diffraction patterns. Thus, we propose that the precursor molecules decompose by (presumably surface) intermolecular elimination of $^tBuSS^tBu$ and subsequent formation of an amorphous film of composition In_2S. Since the molecule's In_2S_2 core has thus been disrupted and this amorphous film has no memory of the molecular precursor's structure, the thermodynamically stable rhombohedral phase crystallizes out of the film.

We [26] and others [27] have demonstrated that β-hydride elimination is a major contribution to the decomposition pathways of alkyl compounds of the Group 13 metals. We proposed therefore that the decomposition and subsequent film growth of the precursors $[R_2In(\mu\text{-}S^tBu)]_2$ would be significantly altered by the absence of β-hydrides in the indium bound alkyl. This is indeed observed.

Although the films deposited at 300°C from $[Me_2In(\mu\text{-}S^tBu)]_2$ (**3**) have a similar elemental composition to those grown from the n-butyl and tert-butyl derivatives, the films are amorphous and contain significant carbonaceous surface residue. At high deposition temperatures (400°C), there is an obvious divergence in the decomposition mechanisms. This is clearly indicated by the growth of In/In_2S_3 films from **3** but tetragonal In_2S_2 film from **1** and **2**. We propose that instead of ligand loss and the deposition of the In_2S_2 core as is seen for **1** and **2**, the lack of a suitable β-hydride elimination pathway, and the increased strength of the In–Me bond in **3** results in core fragmentation and the deposition of an amorphous film with a composition of InS. However, under the conditions of deposition crystallization occurs to give In_2S_3. A similar result is found for films grown from $[(^tBuS)MeIn(\mu\text{-}S^tBu)]_2$ (**4**), see below.

So why is it that lower deposition temperatures produce fragmentation of the In_2S_2 molecular core, while at higher temperatures the core is retained? We believe that despite the counter-intuitive nature of this observation, it may readily be explained in terms of surface catalyzed *versus* gas phase decomposition. If we consider the high temperature deposition as the simplest case, Cowley and co-workers have previously proposed that their dimeric gallium arsenido compounds $[R_2Ga(\mu\text{-}AsR'_2)]_2$ decompose cleanly to yield the Ga_2As_2 core and the appropriate hydrocarbon side products [28]. We may propose a similar mechanism for the decomposition of **1** and **2** at 400°C, resulting in the retention of the In_2S_2 units. At lower deposition temperatures, however, insufficient thermal energy is imparted to the molecule and it undergoes chemisorption with decomposition. The $^tBuSS^tBu$ is thus formed by the elimination of surface bound ^tBuS groups. Similar surface mediated elimination reactions have been observed previously in hydrocarbon systems.

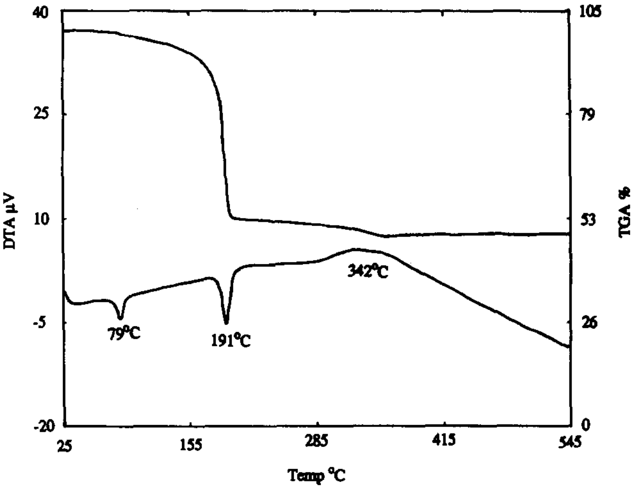

Fig. 6. Thermogravimetric analysis (TGA, upper trace, right hand axis) and differential thermal analysis (DTA, lower trace left hand axis) of $[(^tBuS)MeIn(\mu\text{-}S^tBu)]_2$ (**4**), see text for discussion.

As discussed above, the use of the mono-thiolate complexes (**1**–**3**) as precursors for deposition below 350°C results in films having a low sulfur content, as a consequence of loss of $^tBuSS^tBu$. It is reasonable to propose that if this decomposition pathway is a constant for dimeric alkylindium thiolate compounds, then we may assume that the decomposition of a bis-thiolate complex should yield stoichiometric InS below 350°C.

Thermogravimetric analysis data (Fig. 6) indicates that $[(^tBuS)MeIn(\mu\text{-}S^tBu)]_2$ (**4**) melts at 79°C and subsequently decomposes in two steps, 191°C and 342°C. The final mass loss 51.8% is equivalent to loss of all organic ligands and formation of InS (calculated 52.3% mass loss). Analysis of the effluent gases by ^1H NMR shows that $^tBuSS^tBu$, $H_2C{=}CMe_2$ and CH_4 are the only volatile products observed (eqn. (4)).

$$\left[(^tBuS)MeIn(\mu\text{-}S^tBu)\right]_2 \xrightarrow[350°C]{\Delta}$$

$$2\ InS + {}^tBuSS^tBu + 2\ H_2C{=}CMe_2 + 2\ CH_4 \quad (4)$$

While the formation of $^tBuSS^tBu$ clearly results from the elimination of ^tBuS moieties, the production of isobutene and methane may be accounted for in two ways. Firstly, the loss of the methyl group and one of the sulfur bonded tert-butyl groups may occur independently due to radical cleavage; the organic radicals thus formed undergoing subsequent reaction to give neutral products isolated [26]. Such a decomposition pathway has been previously observed for both Groups 13 and 16 organo substituted compounds [29]. Secondly, a concerted intramolecular elimination of iso-butene and methane may be possible in which the β-hydrogen on the thiol tert-butyl group interacts directly with the indium-methyl via a six-membered cyclic transition state (*e.g.*, **I**). A similar scheme has been proposed by Cowley *et al.* for the decomposition of $[Me_2Ga(\mu\text{-}As^tBu_2)]_2$ [28].

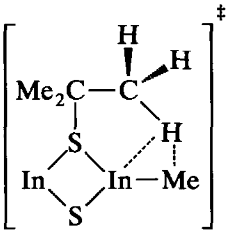

(I)

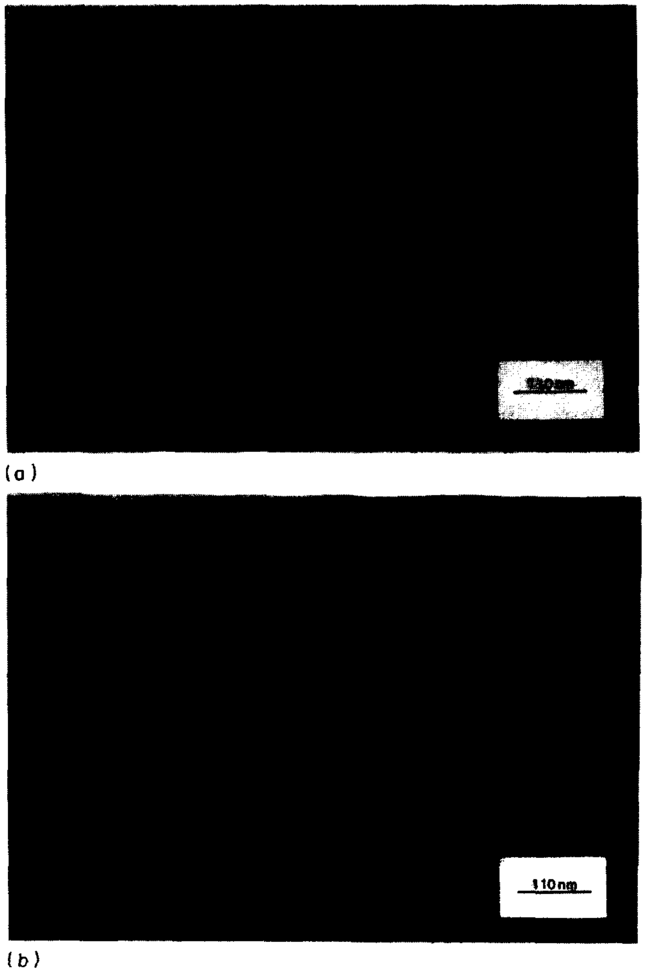

Fig. 7. Bright-field TEM image of films grown from $[(^tBuS)MeIn(\mu\text{-}S^tBu)]_2$ (4) at 300°C, before (a) and after (b) electron-beam annealing *in situ*.

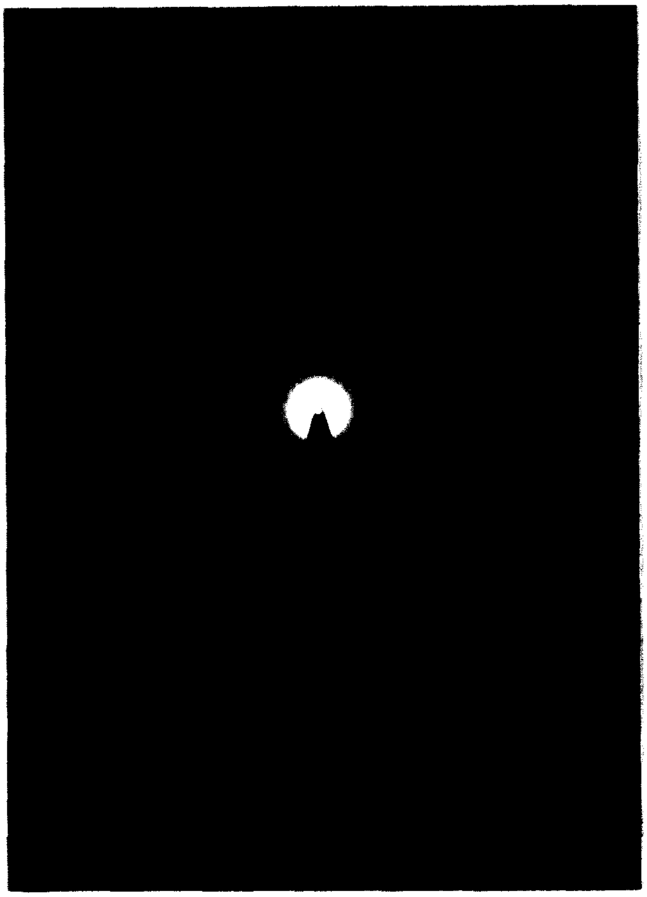

Fig. 8. Selected area diffraction pattern of the annealed films grown from $[(^tBuS)MeIn(\mu\text{-}S^tBu)]_2$ (4), showing the formation of $\beta\text{-}In_2S_3$.

While we have insufficient evidence favoring either mechanism, we note that the two decomposition steps observed in the TGA of 4 are numerically consistent with the stepwise loss of $^tBuSS^tBu$ and tert-butyl radical at 190°C followed by a methyl group at 342°C. Despite the fact that pyrolysis of compound 4 results in the formation of InS, it has insufficient volatility for application as a CVD precursor at atmospheric pressure, however, sublimation occurs readily under vacuum (10^{-3} Torr) and we have thus investigated the use of 4 as a precursor in low pressure MOCVD.

Films deposited from the sulfur rich precursor 4 at a room temperature of 300°C under vacuum are shown as Figs. 7a and 7b. The as-deposited films (Fig. 7a) displayed small island growths on a generally featureless background. On closer inspection these islands were observed to evaporate on focusing of the electron-beam and so were judged to be condensate contamination occurring in the deposition chamber. These films yielded amorphous electron diffraction patterns and gave a composition of 50% In:50% S by EDX analysis. Figure 7b shows the result of focusing the electronbeam on the sample for a short period of time (*i.e.*, annealing the sample *in situ*). Dark precipitates can clearly be observed which yield a diffraction pattern (Fig. 8) consistent with β-In_2S_3 (JCPDS#32-456). This residual area is still of general composition 50% In and 50% S by EDX.

3. Conclusion

We have demonstrated that highly oriented thin films of single phase indium sulfide InS may be grown by MOCVD using the single-source precursors $[(^t\text{Bu})_2\text{In}(\mu\text{-S}^t\text{Bu})]_2$ and $[(^n\text{Bu})_2\text{In}(\mu\text{-S}^t\text{Bu})]_2$. In addition, we have shown that the deposited phase is that of the tetragonal high pressure phase and not the thermodynamically stable rhombohedral phase. This result suggests that the phase of a deposited film may be controlled by the molecular design of the precursor. However, the successful formation of a single phase is highly dependent on the deposition temperature. Thus, while deposition at 400°C gives tetragonal InS, between 300°C and 350°C a change in the growth regime is observed, producing an indium-rich film consisting of orthorhombic InS and an amorphous indium rich phase. The choice of the non β-hydrogen containing methyl ligand on indium, *i.e.*, $[\text{Me}_2\text{In}(\mu\text{-S}^t\text{Bu})]_2$, further changes the decomposition pathway and thus the resultant phase composition.

The loss of sulfur in the deposition of films at 350°C, and below, may be overcome by modification of the molecular design of the precursors. This is enabled by the inclusion of a second "sacrificial" thiolate ligand, in $[(^t\text{BuS})\text{MeIn}(\mu\text{-S}^t\text{Bu})]_2$, designed to be eliminated as $^t\text{BuSS}^t\text{Bu}$, the product responsible for sulfur loss. While this molecular design results in films of equimolar indium : sulfur composition to be deposited, the only crystalline phase observed (albeit on electron-beam heating) is β-In_2S_3.

We may conclude from this study that, while molecular design has allowed for a non-equilibrium phase of InS to be deposited as thin films by MOCVD, and provides a method whereby the loss of sulfur during low temperature deposition may be circumvented, molecular design has at present not allowed the growth of crystalline single phase thin films of rhombohedral InS. We propose, however, that increased understanding of the intimate mechanism of precursor decomposition and thin film crystal growth may provide sufficient information for further modifications towards the design of successful single source precursors for rhombohedral InS. Until such time, this study acts to demonstrate that the simplistic approach to molecular design of single-source precursors for solid state materials so often promoted in the literature is fraught with pitfalls.

4. Experimental section

Thermogravimetric analyses were obtained on a Seiko 200 TG/DTA instrument using an argon carrier gas. Mass spectra were obtained by using a JEOL AX-505H mass spectrometer and associated data system. An electron beam energy of 70 eV was used for EI mass spectra, with a mass resolution of 1500. Ammonia was used as a reagent gas for CI mass spectra. Reported m/z values are for the predominant ion within the isotope pattern for each signal. IR spectra (4000–400 cm^{-1}) were recorded on a Nicolet 5ZDX-FTIR spectrometer between KBr disks; frequencies are reported in cm^{-1}. ^{1}H and ^{13}C NMR spectra were obtained on a Bruker AM-500 spectrometer, and chemical shifts (δ) in ppm are reported relative to SiMe_4 in C_6D_6. Solution molecular weights were determined in pentane using an apparatus similar to that described by Clark [30]. XPS was performed on a Surface Science Instruments Spectrometer (Model SSX-100) with a monochromatized Al K_α source. The spectra were acquired with a 50 eV pass energy and a 1000 μm spot size. All samples were sputtered with 3 keV Argon ions prior to data collection to remove adventitious carbon. All spectra were charge referenced independently to graphite carbon ($\text{C}_{1s} = 284.8 \pm 0.1$ eV), and gold ($\text{Au}_{4f} = 84.0 \pm 0.1$ eV). TEM, and associated EDX analysis, was performed on a Philips EM-420 analytical electron microscope operating at 120 kV.

Unless otherwise stated all manipulations were carried out under a nitrogen atmosphere. Solvents were dried over sodium under nitrogen, and degassed prior to use. ^{t}BuSH (Aldrich) and InMe_3 (Morton) were commercial samples, and were used without further purification. $\text{In}(^n\text{Bu})_3$ and $[(^t\text{Bu})_2\text{In}(\mu\text{-S}^t\text{Bu})]_2$ were prepared according to literature procedures [31,4].

4.1. $[(^n\text{Bu})_2\text{In}(\mu\text{-S}^t\text{Bu})]_2$ (2)

To a pentane solution of $\text{In}(^n\text{Bu})_3$ (2.0 g, 6.98 mmol) was added a slight excess of ^{t}BuSH (*ca.* 1.0 ml, 8.87 mmol) via syringe. The solution was allowed to stir at room temperature for 1 h. All volatiles were removed under vacuum (*ca.* 10^{-2} mmHg) at room temperature to yield a colourless liquid. Yield *ca.* 100%. Molecular weight (pentane): Found 650. Calcd for $[(^n\text{Bu})_2\text{In}(\mu\text{-S}^t\text{Bu})]_2$ 637. Mass spectrum: m/z (CI, NH_3, %) 958 (3M^+, 5%), 896 ($3\text{M}^+ - \text{Bu}$, 20%), 864 ($3\text{M}^+ - \text{S}^t\text{Bu}$, 30%), 595 ($2\text{M}^+ - {}^t\text{Bu} + \text{NH}_3$, 25%), 578 ($2\text{M}^+ - {}^t\text{Bu}$, 15%), 563 ($2\text{M}^+ - \text{S}^t\text{Bu} + \text{NH}_3$, 100%), 546 ($2\text{M}^+ - \text{S}^t\text{Bu}$, 100%), 263 ($\text{M}^+ - {}^t\text{Bu}$, 20%), 246 ($\text{M}^+ - \text{S}^t\text{Bu} + \text{NH}_3$, 15%), 229 ($\text{M}^+ - \text{S}^t\text{Bu}$, 5%). NMR: ^{1}H 1.88, 1.49 (16H, m, $\text{InCH}_2(\text{C}H_2)_2$], 1.37 [18H, s, $\text{SC}(\text{C}H_3)_3$], 1.21 (8H, t, $\text{InC}H_2$) 1.00 [12H, t, $\text{In}(\text{CH}_2)_3\text{C}H_3$]. ^{13}C 49.97

$[\mathrm{S}\mathit{C}(\mathrm{CH}_3)_3]$, 40.94 $[\mathrm{SC}(\mathit{C}\mathrm{H}_3)_3]$, 35.51, 33.77 $(\mathrm{InCH}_2\mathit{C}\mathrm{H}_2\mathit{C}\mathrm{H}_2)$, 25.34 $(\mathrm{In}(\mathrm{CH}_2)_3\mathit{C}\mathrm{H}_3)$, 19.85 $(\mathrm{In}\mathit{C}\mathrm{H}_2)$. IR (neat): 2970–2700 (s), 1457s, 1416w, 1364s, 1337w, 1289w, 1260w, 1250w, 1213w, 1160w, 1061w, 1015w, 958w, 867w, 815w, 662m, 632sh, 577m, 486w.

4.2. *$[\mathrm{Me}_2\mathrm{In}(\mu\text{-}\mathrm{S}^t\mathrm{Bu})]_2$ (3)*

To a pentane (*ca.* 30 ml) solution of InMe_3 (2.0 g, 12.5 mmol), at room temperature, was added via syringe a slight excess of $^t\mathrm{BuSH}$ (1.5 ml, 13.3 mmol). Vigorous evolution of gas was observed during the addition. After stirring for *ca.* 0.5 h all volatiles were removed under vacuum to leave a white solid. This was recrystallized from the minimum of fresh pentane (*ca.* 20 ml) at −25°C overnight. Yield 92%, m.p. 80–81°C. Molecular weight (pentane): Found 505, Calcd for $[\mathrm{Me}_2\mathrm{In}(\mu\text{-}\mathrm{S}^t\mathrm{Bu})]_2$ 468. Mass spectrum: *m/z* (EI, %) 685 ($3\mathrm{M}^+ - \mathrm{Me}$, 30%), 452 ($2\mathrm{M}^+ - \mathrm{Me}$, 100%), 396 ($2\mathrm{M}^+ - {}^t\mathrm{Bu} - \mathrm{Me}$, 20%), 218 ($\mathrm{M}^+ - \mathrm{Me}$, 10%), 163 (MeInS, 35%), 145 ($\mathrm{Me}_2\mathrm{In}$, 80%), 115 (In, 65%). NMR: $^1\mathrm{H}$ 1.31 [18H, s, $\mathrm{SC}(\mathrm{C}\mathit{H}_3)_3$], 0.31 (12H, s, $\mathrm{InC}\mathit{H}_3$). $^{13}\mathrm{C}$ 46.36 $[\mathrm{S}\mathit{C}(\mathrm{CH}_3)_3]$, 35.92 $[\mathrm{SC}(\mathit{C}\mathrm{H}_3)_3]$, −2.28 $(\mathrm{In}\mathit{C}\mathrm{H}_3)$. IR (Nujol): 1212w, 1155s, 1024w, 928w, 812w, 704s, 571s, 505s, 477s, 419m, 380m.

4.3. *$[(^t\mathrm{BuS})\mathrm{MeIn}(\mu\text{-}\mathrm{S}^t\mathrm{Bu})]_2$, (4)*

$[(\mathrm{Me})_2\mathrm{In}(\mu\text{-}\mathrm{S}^t\mathrm{Bu})]_2$ (0.5 g, 1.06 mmol) was refluxed in neat $^t\mathrm{BuSH}$ (*ca.* 30 ml, 266.0 mmol) overnight. The next day all volatiles were removed under vacuum leaving an oily white residue. This was recrystallized from the minimum of pentane (*ca.* 10–20 ml) to give a white crystalline product. Mp 77–78°C. Molecular weight (pentane): Found 590, Calcd for $[(^t\mathrm{BuS})\mathrm{MeIn}(\mu\text{-}\mathrm{S}^t\mathrm{Bu})]_2$ 616. Mass spectrum: (EI, %): 527 ($2\mathrm{M}^+ - \mathrm{S}^t\mathrm{Bu}$, 100%). (CI, %): 909 ($3\mathrm{M}^+ - \mathrm{Me}$, 15%); 835 ($3\mathrm{M}^+ - \mathrm{S}^t\mathrm{Bu}$, 100%), 761 [$\mathrm{In}_3\mathrm{Me}_4(\mathrm{S}^t\mathrm{Bu})_4$, 100%], 527 ($2\mathrm{M}^+ - \mathrm{S}^t\mathrm{Bu}$, 40%). NMR: $^1\mathrm{H}$ 1.49 [18H, s, $\mathrm{SC}(\mathrm{C}\mathit{H}_3)_3$], 0.62 [3H, s, $\mathrm{InC}\mathit{H}_3$]. $^{13}\mathrm{C}$ 46.57 $[\mathrm{S}\mathit{C}(\mathrm{CH}_3)_3]$, 36.83 $[\mathrm{SC}(\mathit{C}\mathrm{H}_3)_3]$, 1.41 $(\mathrm{In}\mathit{C}\mathrm{H}_3)$. IR (Nujol): 1263w, 1210m, 1154s, 1024m, 928w, 812m, 717s, 566s, 502s, 423m, 384s.

4.4. *Chemical vapor deposition studies*

Depositions were carried out at various temperatures (nominally 290°C, 350°C and 400°C) in an atmospheric pressure laminar-flow hot wall glass reactor, as previously described [5]. Argon was purified using a $\mathrm{Cr}/\mathrm{Cr}_2\mathrm{O}_3$ purifier prior to entry into the chamber. Depositions were carried out on p-type (100) oriented silicon and KBr single crystal substrates. No appreciable difference in film morphology as a function of substrate was noted. The CVD chamber was loaded with substrates and was heated and purged with argon for *ca.* 1 h prior to deposition. The solid precursors (**1** and **3**) were placed in the mouth of the chamber over a hot plate, as described in ref. 5. The liquid precursor (**2**) was placed in an external bubbler and heated with an oil bath. The flow rate of carrier gas (Argon) was between 0.5–1 l min^{-1} through the resistively heated deposition zone. Outflow from the reaction chamber exited to an oil bubbler via two cold traps (*ca.* −80°C, acetone/dry ice), which were used to trap out any volatiles produced from the CVD process.

Further studies using $[(^t\mathrm{Bu})_2\mathrm{In}(\mu\text{-}\mathrm{S}^t\mathrm{Bu})]_2$ (**1**) and $[(^t\mathrm{BuS})\mathrm{MeIn}(\mu\text{-}\mathrm{S}^t\mathrm{Bu})]_2$ (**4**) as precursors, were carried out using a vacuum reactor similar to that described recently by Maverick *et al.* [32]. A vertical cold-wall reactor was used at *ca.* 10^{-2}–10^{-3} Torr. The substrates were attached to a glass probe and heated to the described temperature using an infra-red heater. The precursors were warmed to between 60–70°C (10^{-2} Torr) as required for sublimation of the compound. No decomposition of **1** was observed at this temperature, in contrast to our studies at atmospheric pressure [4].

Acknowledgments

The National Research Council and NASA Lewis Research Center are gratefully acknowledged for a Post-doctoral Fellowship to MBP. Financial support for this work is provided by the National Science Foundation and the Aluminum Research Board. We are indebted to Dr. A.N. Tyler for assistance with the mass spectrometry measurements. We thank Prof. Alan Cowley for the invitation to take part in this symposium.

References

1 For recent review articles see: (a) A. C. Jones, *Chemtronics*, 4 (1989) 15; (b) D. C. Bradley, *Chem. Rev.*, *89* (1989) 1317; (c) A. H. Cowley and R. A. Jones, *Angew. Chem., Int. Ed. Engl.*, *28* (1990) 1208; (d) G. S. Girolami and J. E. Gozum, *Mater. Res. Soc. Symp. Proc.*, *168* (1990) 319.

2 B. S. Meyerson, F. K. LeGoues, T. M. Nguyen and D. L. Harame, *Appl. Phys. Lett.*, *50* (1987) 113.

3 A. N. MacInnes, M. B. Power and A. R. Barron, *Chem. Mater.*, *4* (1992) 11.

4 A. N. MacInnes, W. M. Cleaver, A. R. Barron, M. B. Power and A. F. Hepp, *Adv. Mater. Opt. Electron.*, *1* (1992) 229.

5 C. C. Landry, L. K. Cheatham, A. N. MacInnes and A. R. Barron, *Adv. Mater. Opt. Electron.*, *1* (1992) 3.

6 P. M. Jeffries and G. S. Girolami, *Chem. Mater.*, *1* (1989) 8.

7 R. G. Gordon, J. Prosid, F. B. Ellis, Jr. and A. E. Delahoy, *Solar Energy Materials*, *18* (1989) 263.

8 W. S. Rees, Jr. and C.R. Caballero, *Adv. Mater. Opt. Electron*, *1* (1992) 59.

9 (a) T. Nishino and Y. Hamakawa, *Jpn. J. Appl. Phys.*, *16* (1977) 1291; (b) R. S. Becker, T. Zheng, J. Elton and M. Saeki, *Sol. Energy Mater.*, *13* (1986) 97.

10 (a) W.-T. Kim and C. -D. Kim, *J. Appl. Phys.*, *60* (1986) 2631; (b) R. Nomura, K. Kanaya, A. Moritake and H. Matsuda, *Thin Solid Films*, *167* (1988) L27.

11 R. Iyer, R. R. Chang and D. L. Lile, *Appl. Phys. Lett.*, *53* (1988) 134.

12 A. N. MacInnes, M. B. Power, A. R. Barron, P. P. Jenkins and A. F. Hepp, *Appl. Phys. Lett.*, *62* (1993) 711.

13 A. N. MacInnes, M. B. Power and A. R. Barron, unpublished results.

14 R. Nomura, S.-J. Inazawa, K. Kanaya and H. Matsuda, *Polyhedron, 8* (1989) 763.

15 J. H. Rogers, A. W. Apblett, W. M. Cleaver, A. N. Tyler and A. R. Barron, *J. Chem. Soc., Dalton Trans.*, (1992) 3179.

16 (a) A. Storr and B. S. Thomas, *J. Chem. Soc. A*, (1971) 3850; (b) F. C. Sauls, C. L. Czekaj and L. V. Interrante, *Inorg. Chem.*, *29* (1990) 4688.

17 M. B. Power, W. M. Cleaver, A. W. Apblett, A. R. Barron and J. W. Ziller, *Polyhedron, 11* (1992) 477.

18 See for example, T. L. Brown, *Acc. Chem. Res.*, *1* (1968) 23.

19 K. Schubert, E. Dörre and E. Günzel, *Naturwissenschaften, 41* (1954) 488.

20 S. Kabalkina, V. G. Losev and N. M. Gasanly, *Solid State Commun.*, *44* (1982) 1383.

21 C. D. Wagner, L. H. Gale and R. H. Raymond, *Anal. Chem.*, *51* (1979) 466.

22 C. D. Wagner, in D. Briggs (ed.), *Handbook of X-ray and U.V. Photoelectron Spectroscopy*, Heydon, London, 1977, Chap. 7.

23 F. Klanberg and H. Spandan, *J. Inorg. Nuclear Chem.*, *19* (1961) 180.

24 (a) A. Thiel and H. Luckmann, *Z. anorg. Chem.*, *172* (1928) 353; (b) W. Klemm and H. U. von Vogel, *Z. anorg. Chem.*, *219* (1934) 45.

25 W. J. Duffin and J. H. C. Hogg, *Acta Cryst.*, *20* (1966) 566.

26 (a) W. M. Cleaver, A. R. Barron, Y. Zhang and M. Stuke, *Appl. Surface Sci.*, *54* (1992) 8; (b) Y. Zhang, W. M. Cleaver, M. Stuke and A. R. Barron, *Appl. Phys. A.*, *55* (1992) 261.

27 D. K. Russell, *Coord. Chem. Rev.*, *112* (1992) 131 and references therein.

28 A. H. Cowley, B. L. Benac, J. G. Ekerdt, R. A. Jones, K. B. Kidd, J. Y. Lee and J. E. Miller, *J. Am. Chem. Soc.*, *110* (1988) 6248.

29 Y. Zhang and M. Stuke, *Chemtronics, 4* (1989) 71.

30 E. P. Clark, *Ind. Eng. Chem., Anal. Ed.*, *13* (1941) 820.

31 R. Nomura, S.-J. Inazawa, H. Matsuda and S. Saeti, *Polyhedron, 6* (1987) 507.

32 R. Kumar, F. R. Fronczek, A. W. Maverick, W. G. Lai and G. L. Griffin, *Chem. Mater.*, *4* (1992) 577.